

Development and calibration of pyroelectric radiometer standards at NIST

G. P. Eppeldauer, J. Zeng, and L. M. Hanssen
Optical Technology Division
National Institute of Standards and Technology
Gaithersburg, Maryland 20899

ABSTRACT

The reference spectral power responsivity scale of NIST is being extended from the silicon range to the infrared (IR) using pyroelectric radiometers. Two transfer standard pyroelectric radiometers have been developed at NIST. The main design consideration was to obtain only a minimal increase in the measurement uncertainty during the responsivity scale extension. Domain engineered LiNbO₃ and regular LiTaO₃ pyroelectric detectors were used in the two radiometers. Both detectors are gold-black coated and temperature controlled. Reflecting domes are attached to the radiometer inputs to decrease the reflectance loss and to improve the spatial uniformity of responsivity in the infrared. Four commercial pyroelectric detectors have been added to the group and used as working standards. The relative spectral responsivity of all pyroelectric detectors was determined from spectral reflectance measurements. The radiant power responsivity tie points were derived from Si trap and single element detectors traceable to the NIST reference responsivity scale. The pyroelectric radiometers have been characterized for frequency and temperature dependent responsivity, noise, spatial non-uniformity of responsivity, angular responsivity, and linearity. The expanded (relative) uncertainty of the spectral power responsivity calibrations ranged between 0.5 % and 1.2 % ($k=2$) within the 1 μm to 19 μm range.

1. INTRODUCTION

Infrared detector standards are being developed for the 2 to 2.5 μm [1], the 3 to 5 μm [2], [3], and the 8 to 12 μm [4] atmospheric windows where the absorption lines will not affect the uncertainty of the responsivity measurements. The present work describes the development of pyroelectric transfer standard radiometers and also the use of commercially available pyroelectric detectors.

The pyroelectric transfer standard radiometers were primarily developed to extend the reference radiant power responsivity scale from the end of the silicon wavelength range at 1 μm to the 8 to 12 μm range (and beyond) with the lowest possible measurement uncertainty. It was shown earlier that gold-black coated domain engineered LiNbO₃ pyroelectric detectors can be applied for responsivity measurements with about 0.1 % ($k=1$) responsivity uncertainty in the near infrared range [5]. As increased reflectance in the longer wavelength infrared results in increased non-uniformity of the spatial responsivity [1], reflecting domes are mounted at the inputs to minimize reflection losses [6], [7]. The commercial pyroelectric detectors are used as working standard radiometers to propagate the NIST infrared responsivity scale to different applications.

2. RADIOMETER DESIGN

The radiometers were designed and selected with optimum radiometric and electronic characteristics to minimize the increase in the uncertainty of spectral responsivity associated with transfer calibrations.

2.1. Transfer standard radiometers

The two transfer standard radiometers contain 1-cm diameter pyroelectric detector elements with gold-black coatings used to convert optical power into temperature change and then into current. In Radiometer #2, a domain-engineered LiNbO₃ detector and in Radiometer #1, a regular LiTaO₃ detector without domain engineering were used [5]. Each detector was extended to a radiometer. As it is shown in Fig. 1, the detector-case is attached to a thermoelectric (TE) cooler/heater and a thermistor, mounted inside of the detector case, is used as a temperature sensor. Using a temperature

controller, the temperature of the detector is controlled to a constant value slightly above room temperature. The gold coated reflecting dome has a hemisphere shape, with an internal diameter of 33 mm. It is mounted above the 20° tilted pyroelectric detector. The dome has a 4 mm diameter opening at the optical axis. The figure shows how the specular components from a parallel incident radiation at the two ends of the input beam diameter are reflected back to the active area of the detector. A current-to-voltage converter with multiple signal-gain selections is mounted in an Aluminum box. The box is attached to the radiometer Aluminum housing using a connector. The overall housing of the radiometer is electrically shielded to minimize 60 Hz pickup. A photo of the radiometer is shown in Fig. 2.

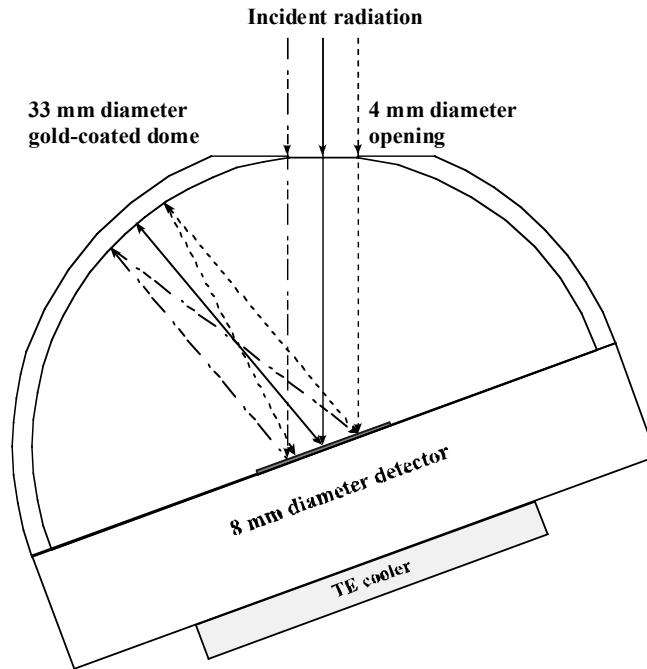


Fig. 1. Input scheme of the transfer standard pyroelectric radiometer.

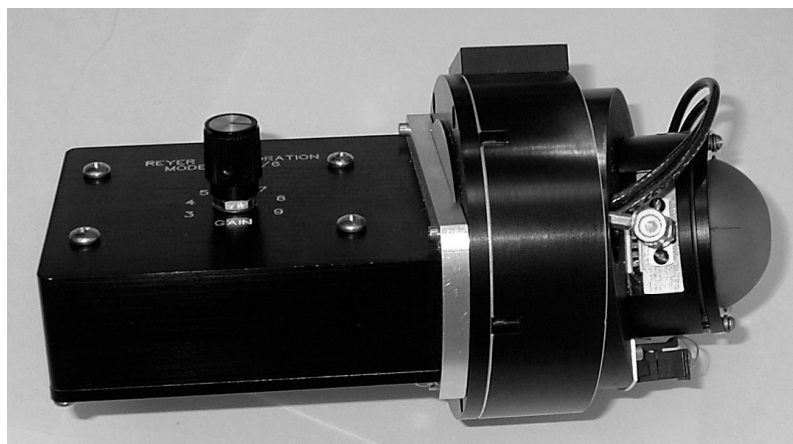


Fig. 2. Photo of the transfer standard pyroelectric radiometer (the top cover is removed)

2.2. Working standard radiometers

Four commercial pyroelectric detectors are used as working standards. These working standards propagate the NIST infrared responsivity scale to different field applications. All four detectors are mounted in a housing where the detector temperature is monitored. The preamplifier is located inside the detector can where a fixed 10 G Ω feedback resistor is connected to an operational amplifier to convert the detector current into an output voltage. The detectors are coated with a black paint to convert optical radiation changes into temperature changes.

3. RADIOMETER CHARACTERIZATION

A set of characterizations were performed on the radiometers to establish the uncertainties associated with the radiometer's responsivity during both calibration and the calibration-transfer to other radiometers. The frequency- and temperature-dependent responsivity, signal-gain stability, and noise characteristics were measured in the Ambient Infrared Detector Characterization Facility. The Infrared Detector Evaluation Facility (IDEF) was used for measurement of the spatial non-uniformity of responsivity, linearity, angular responsivity, absolute responsivity, stability, and repeatability. The Infrared Total Integrated Scatter Instrument (ITIS) was used to measure the reflectance at laser wavelengths. The Fourier Transform Infrared Spectrophotometry Facility (FTIS) was used to measure the spectral reflectance of the coated detectors to determine the relative spectral responsivity.

3.1. Characterization of the transfer standard radiometers

The detector-dome combination acts as a trap to provide near unity absorptance across the entire wavelength range of use. Accordingly, the spatial uniformity of responsivity at long wavelengths is significantly improved over the bare detector case. The spatial scan results obtained for Radiometers #1 and #2 at 10.6 μm are shown in Fig. 3. The size of the scanning spot was 0.2 mm. The maximum-to-minimum spatial non-uniformity of responsivity is less than 0.6 % within a 1.5 mm diameter center area of both radiometers. Without the reflecting dome, the spatial non-uniformity of responsivity was found to be 10 % to 15 % at 10.6 μm .

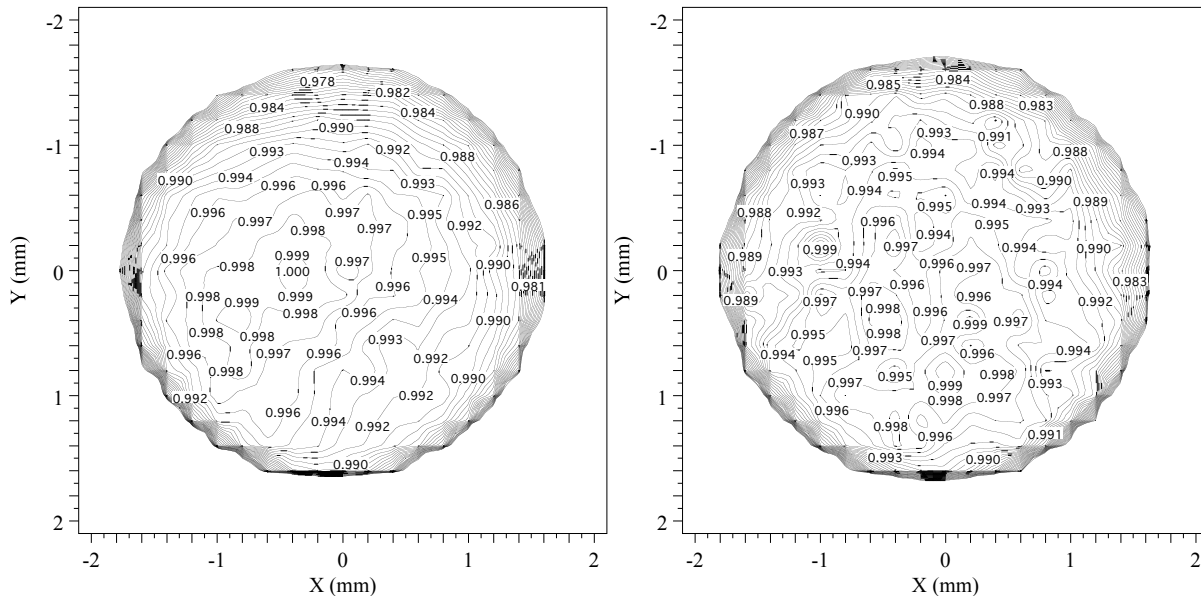


Fig. 3. Spatial (normalized) uniformity of responsivity of the dome-equipped transfer standard pyroelectric Radiometers #1 (left plot) and #2 (right plot) at 10.6 μm .

The noise equivalent power (NEP) is one of the most important characteristics of pyroelectric radiometers that are used to measure 1 μ W signal levels from monochromators. Therefore, the noise characteristics of the two transfer standard radiometers were tested. Fig. 4 shows the measured output total noise of the domain engineered Radiometer (#2) on the left Y axis. The 1/f noise of the operational amplifier is the dominating noise up to a gain of 10^6 V/A. At higher gain levels the resistor (parallel connected detector resistance and feedback resistance) noise dominates the output noise of the radiometer. The background produced photocurrent and its noise are negligibly small because of the very low responsivity (output photocurrent per input radiant power) of the pyroelectric detector (about six orders of magnitude lower than that of silicon photodiodes). This means that pyroelectric detectors do not operate in background limited condition as most of the high responsivity infrared detectors do. Because of the very low detector responsivity, the signal power to be measured has to be very high. While radiant power levels of 1 pW with a signal-to-noise (S/N) ratio of 100 or higher can be measured with silicon photodiodes, the radiant power for pyroelectric detectors must be about six orders of magnitude higher to get similar photocurrents and S/N ratios. The noise equivalent current (NEC) is calculated as the ratio of the output total noise voltage to the signal gain. The NEC is shown on the right Y axis. The noise measurements were made both in the dark and at 1.5 pA signal current originating from the chopped signal of a ceramic glower. The chopping frequency was 10.5 Hz and the lock-in time constant was 1 s. Each data point was obtained as the standard deviation of the mean from 20 measurements. The same output total noise voltage (as in Fig. 4) was measured for both cases with a relative measurement uncertainty of 25 % ($k=1$). The NEC at a signal gain of 10^9 V/A is 6.5 fA. An NEP of 20 nW can be calculated as the ratio of the 6.5 μ V output total noise (at 10^9 V/A) to the 326 V/W responsivity of this radiometer at 1.32 μ m and a 1 s lock-in time constant. The radiometer responsivity was measured by substitution against a Ge detector standard in a measurement of total power in the beam from a 1.32 μ m diode laser. The 1 s time constant corresponds to a frequency bandwidth of 0.16 Hz. The NEP expressed for a 1 Hz electrical bandwidth is:

$$\text{NEP} = 20 \text{ nW} \times (1/0.16)^{1/2} = 50 \text{ nW/Hz}^{1/2}.$$

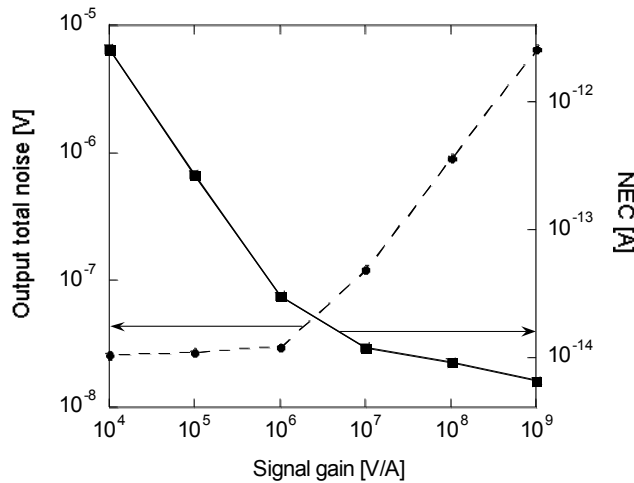


Fig. 4. Noise characteristics of the domain engineered LiNbO₃ pyroelectric Radiometer #2.

The change of the NEP at a signal-gain of 10^9 V/A versus lock-in time constant is shown in Fig. 5 for the regular LiTaO₃ Radiometer #1. The graph shows that the NEP decreases from 13 nW at a 1 s lock-in time constant to 3 nW at a 10 s time constant. The large decrease in the NEP was obtained because of the 766 V/W responsivity of Radiometer #1 at a gain of 10^9 V/A, which is more than two times higher than that of the domain engineered Radiometer #2 of 326 V/W. (The pyroelectric coefficient of LiNbO₃ is smaller than that of LiTaO₃ and the domain engineered detector is about four times thicker than the regular LiTaO₃.)

The frequency dependent responsivity of the radiometers was measured at a gain of 10^9 V/A. The measured 3 dB upper roll-off frequency was 76 Hz for both transfer standards. This frequency was determined by the 2.1 pF stray capacitance connected in parallel with the $1\text{ G}\Omega$ feedback resistor. In order to have an operating point on the plateau of the frequency dependent responsivity curve, the feedback resistor cannot be increased to a higher value than $10^9\ \Omega$. In this case, chopping frequency of about 10 Hz can be used. Fig. 4 shows that the NEC (and hence the NEP) will decrease if the feedback resistor can be further increased. A feedback resistor of $10\text{ G}\Omega$ could be used if the stray capacitance was decreased by an order of magnitude. In this case, sub 10 nW NEPs could be achieved with a 1 s lock-in time constant.

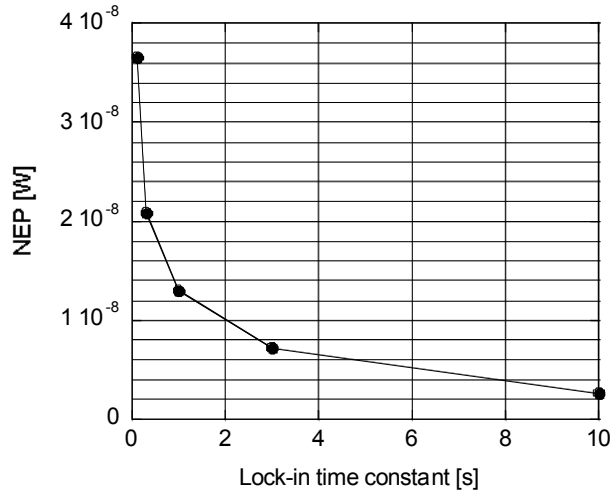


Fig. 5. NEP of the regular LiTaO_3 pyroelectric Radiometer #1 at a signal-gain of 10^9 V/A versus lock-in time constant.

For the two domed pyroelectric transfer standards, the results of the spatial non-uniformity of responsivity measurements together with the reflectance measurement results obtained on the ITIS and FTIS facilities are summarized in Table 1. The FTIS measurement provides the spectral dependence of the reflectance, whereas the ITIS measurement provides a more accurate (absolute reflectance) result, at a single wavelength. The table shows that 0.1 % to 0.2 % reflectance levels were measured on the domed detectors at $10.6\ \mu\text{m}$ with the two different methods. The FTIR reflectance measurement indicated no wavelength dependence (leading to the spectrally flat responsivity seen in Fig. 10). The low reflectance of the domed detector in the infrared range results in the low (0.5 % to 0.6 %) spatial non-uniformity of responsivity at $10.6\ \mu\text{m}$ (as can also be seen in Fig. 3) for both domed detectors.

Table 1. Experimental results of spatial non-uniformity of responsivity and reflectance measurements of the regular pyroelectric Radiometer #1 and the domain engineered pyroelectric Radiometer #2 at $10.6\ \mu\text{m}$

Transfer standard pyroelectric radiometers		Spatial non-uniformity of responsivity	Spectral reflectance (from FTIS)	Reflectance (from ITIS)
#1	Bare	15% (max-min)	16%	—
#1	w/Dome	< 0.6%	—	0.18%
#2	Bare	—	7%	—
#2	w/Dome	< 0.5%	0.1%	0.15%

To obtain the detector element absorptance, we also need to include loss sources other than reflectance: absorption by the dome of the detector reflected radiation, and radiation absorbed outside of the detector. We assume that the gold-coated dome reflectance is $98.5 \pm 0.5\%$. Ray-tracing results indicate that the radiation absorbed outside of the detector is $< 0.05\%$ and $< 0.02\%$, for Radiometers #1 and #2, respectively. Using these measurement results, the absorptance at $10.6\ \mu\text{m}$ is 99.6% and 99.8% , for Radiometers #1 and #2, respectively.

3.2. Characterization of the working standard radiometers

All four working standard radiometers have been fully characterized to operate them under application conditions so that the measurement uncertainty in use will not be significantly higher than when calibrated. The characterizations help the users to determine the optimum spot size of the incident beam, chopping frequency, and temperature dependent responsivity corrections for different applications.

The radiometers were tested for frequency dependent responsivity at the $10^{10}\ \text{V/A}$ (fixed) signal-gain. They measured the radiation from a ceramic glower from chopper frequencies ranging between $4.5\ \text{Hz}$ and $200\ \text{Hz}$. The curve-fit to the measured data is shown for one of the test radiometers in Fig. 6. The fit equation is:

$$y = m_1 \frac{\sqrt{1 + \left(\frac{M_0}{m_4}\right)^2}}{\sqrt{\left[1 + \left(\frac{M_0}{m_2}\right)^2\right] \left[1 + \left(\frac{M_0}{m_3}\right)^2\right]}}$$

where y is the signal gain (signal output / signal input), M_0 is the frequency, m_1 is the magnitude (amplitude) of the DC output voltage, m_4 is a roll-on frequency produced by a differentiating time constant, m_2 and m_3 are roll-off frequencies resulting from integrating time constants. The graph shows that the responsivity roll-on originating from m_4 of the black paint can cancel the responsivity roll-off produced by m_2 of the current-to-voltage converter. The result is a $109\ \text{Hz}$ upper roll-off frequency originating from the remaining m_3 time constant produced by the paint coating.

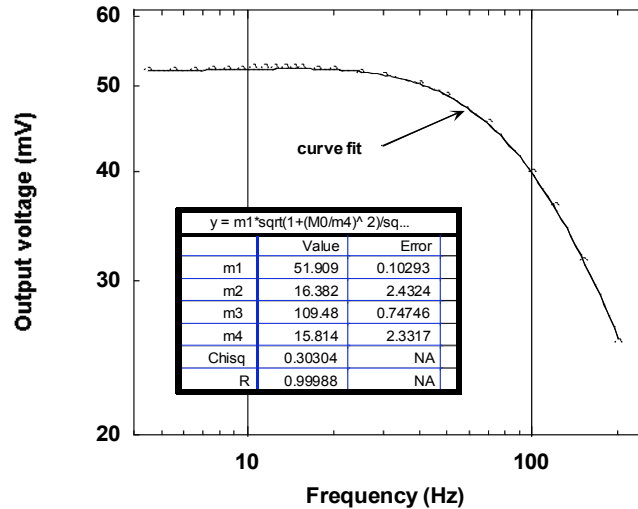


Fig. 6. Frequency dependent responsivity of a working standard pyroelectric radiometer at a signal (current) gain of $10^{10}\ \text{V/A}$.

The spatial non-uniformity of responsivity was measured at $10.6\ \mu\text{m}$. The results in Fig. 7 show that the detector has a roughly 1 % spatial variation of responsivity in the center area which makes it possible to use it in radiant power measurement mode (where the detector is underfilled by the incident radiation) with low uncertainty. The incident radiation should avoid the detector corners, where the responsivity is highly non-uniform because of the contacts.

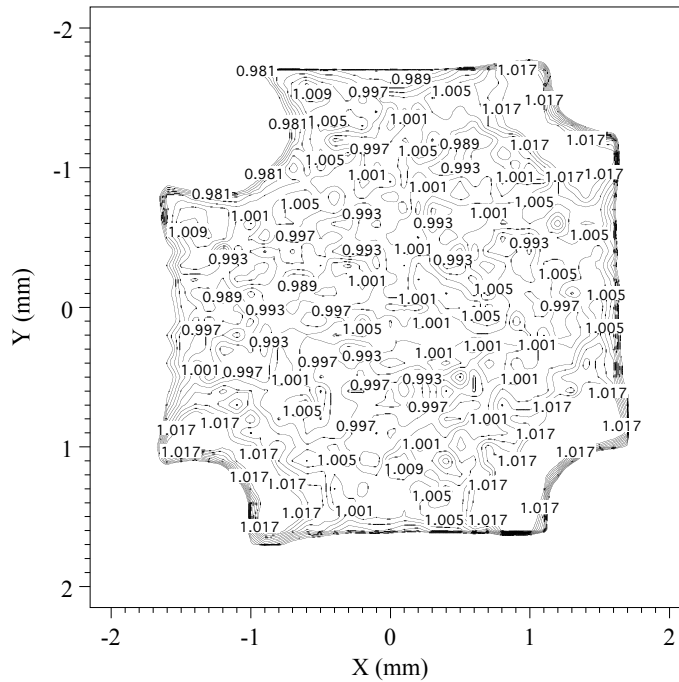


Fig. 7. Spatial non-uniformity of responsivity of one of the paint coated pyroelectric detectors at $10.6\ \mu\text{m}$. The responsivity is highly non-uniform at the corners because of the contacts.

In order to determine the correct responsivity of the radiometers for all future applications, the temperature coefficient of responsivity (the relative responsivity change versus temperature) was measured for all four working standard radiometers. The radiometers were located in a temperature controlled box and measured the stable broad-band radiation from a tungsten lamp (located outside of the box) at different detector (box) temperatures. The slope of the output voltages versus temperature data points (from a linear fit) was divided by the output voltage at the predicted temperature reading of the future absolute responsivity calibration. A $0.19\ \%/^{\circ}\text{C}$ temperature coefficient of responsivity was obtained for three detectors and $0.26\ \%/^{\circ}\text{C}$ was obtained for one detector. The relative expanded uncertainty of these measurements was $20\ \%$ ($k=2$).

The noise floor of the working standard radiometers was measured in the dark at a chopping frequency of $10.5\ \text{Hz}$, with a lock-in integrating time constant of $2\ \text{s}$. The standard deviation was calculated from 32 data points. The calculated noise equivalent photocurrent ranged between $2\ \text{fA}$ and $4\ \text{fA}$. With a $10^{-6}\ \text{A/W}$ nominal responsivity at $10.6\ \mu\text{m}$, a noise equivalent power (NEP) of 2 to $4\ \text{nW}$ was obtained for the working standard radiometers using the $2\ \text{s}$ time constant.

The angular responsivity of the test detectors was measured to obtain quantitative information about responsivity changes when the incident radiation geometry is varied. This enables corrections to be made for any specific geometry, such as for the converging beam from a monochromator. The $10.6\ \mu\text{m}$ laser beam, in both s and then p polarization states, was focused to the working standard radiometers with a biconvex lens. The working standard radiometers were rotated about the detector center (coincident with the input beam). The working standard radiometer output signal was

divided by the signal of the monitor detector. The ratios were recorded versus angle of rotation. Fig. 8 shows the angular response for one of the working standard radiometers at 10.6 μm . The angular response change for the average *s* and *p* polarizations was less than 0.5 % within a $\pm 15^\circ$ angular range.

A radiometer should have constant radiant power responsivity when the power level of the incident radiation changes. The working standard radiometers were measured from the maximum allowed radiant power level down to the low end limit, determined by the signal-to-noise ratio at the test radiometer output.

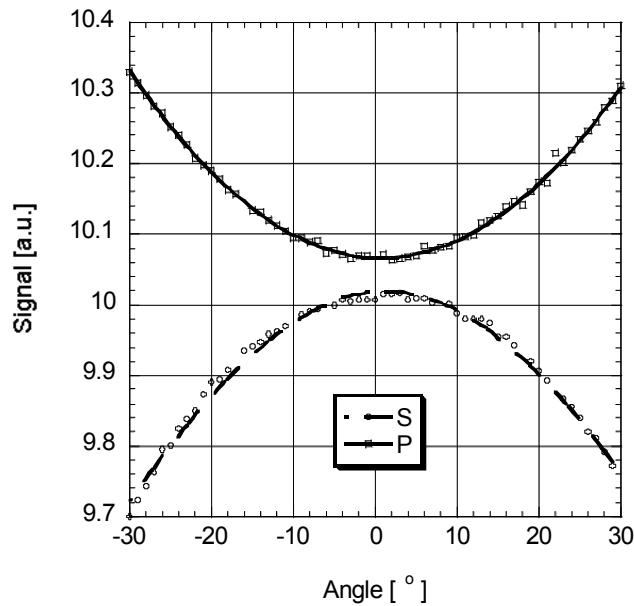


Fig. 8. The angular response of the working standard Radiometer P8 at 10.6 μm .

The response linearity of two working standard radiometers was measured using a collimated beam from a CO₂ laser (tuned to 10.6 μm). The linearity measurement results are shown for both working standard radiometers in Fig. 9. The beam power was adjusted to different power levels at which measurements were made with the same filter, moved in and out of the beam and the ratio or filter transmittance calculated. A constant transmittance (which is proportional to the responsivity) indicates the linearity of the detector response versus incident radiant power. The beam power was changed using ND filters and a polarizer attenuator. The maximum power with the filter out of the laser beam was 3 mW (shown in Fig. 9 with the large open circle). The results show that the working standard radiometers had linear response (constant responsivity) within a power range larger than three orders of magnitude. The small signal-to-noise ratios limited the linearity tests to a minimum incident power of about 0.1 μW .

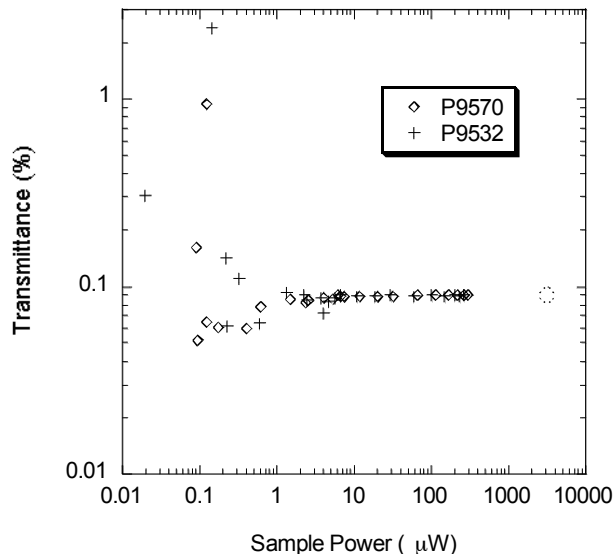


Fig. 9. Linearity measurement results of two working standard radiometers at 10.6 μm .

4. CALIBRATION OF PYROELECTRIC RADIOMETERS

The spectral power responsivities of the transfer and working standard pyroelectric radiometers were determined using the same calibration facilities and similar procedures.

The facility for Spectral Irradiance and Radiance Responsivity Calibrations using Uniform Sources (SIRCUS) made it possible to improve the uncertainty of monochromator-based spectral radiant power responsivity measurements and to extend the calibrations from power mode to irradiance [2] and radiance measurement modes [8]. The high beam power and stability of the tunable IR lasers of the SIRCUS facility makes it possible to calibrate a wide range of IR detectors and radiometers for spectral power, irradiance, and radiance responsivity.

After determination of the relative spectral responsivities using the ITIS and the FTIS facility results, radiant power responsivity tie points were made at a few wavelengths using the IDEF facility to convert the relative spectral responsivities into absolute. The tie points have been derived recently from a Si-trap detector and earlier from a single element Ge photodiode, both traceable to the NIST reference responsivity scale [9]. During the calibration of the first two working standard radiometers, more tie points have been derived from an earlier developed LiNbO_3 pyroelectric radiometer standard [5] and also from a single element LiTaO_3 pyroelectric transfer detector (PD2) calibrated against the primary standard cryogenic radiometer at 10.6 μm [10].

The responsivity tie points were determined using the detector substitution method. The standard detector, having power responsivity s_s , is placed into the laser beam, with its output current y_s measured. A test detector is then placed into the same beam, with its output current y_T measured. The power responsivity of the test detector is then given by

$$s_T = \frac{y_T}{y_s} \cdot s_s$$

The signals y_s and y_T are corrected for the drift of the source intensity by using the monitor detector signal. All measurements were performed at an ambient temperature of $25 \text{ }^\circ\text{C} \pm 1 \text{ }^\circ\text{C}$.

4.1. Transfer standard radiometer responsivities

The spectral power responsivity of the transfer standard pyroelectric Radiometer #2 at a signal gain of 10^9 V/A is shown as an example in Fig. 10 between 1 μm and 18 μm . The relative spectral responsivity function was determined from spectral reflectance measurements on the FTIR. The noise at the short wavelength end of each scan was caused by the small signal-to-noise ratios. The responsivity tie points are shown with open squares and a dot in the center. The absorbances at 10.6 μm (see Section 3.1) were used to determine the 10.6 μm tie point relative to the 785 nm reference tie point. The relative expanded ($k=2$) uncertainties are shown with error bars. The uncertainty of the 785 nm tie point propagated to 10.6 μm together with additional uncertainty components, shown in Table 2, increased the relative expanded uncertainty from 0.46 % to 0.58 % ($k=2$). This is the dominating uncertainty component for the overall spectral power responsivity function of the pyroelectric transfer standard Radiometer #2.

4.2. Working standard radiometer responsivities

As the working standard radiometers propagate the NIST detector responsivity scales to field applications, the increase in the responsivity uncertainty during the scale transfer has to be minimized. For the first two radiometers, a redundant responsivity scale transfer was developed to obtain low and reliable uncertainty of spectral power responsivity.

The initial redundant responsivity scale transfer was made prior to the final calibration of the transfer standard Radiometers #1 and #2, when the Si-trap detector was not available for a low uncertainty tie point at the short wavelength end. The calibration results of the first two working standard pyroelectric radiometers are shown in Fig. 11. The plot shows the FTIS and ITIS determined relative spectral responsivity curves and the (absolute) power

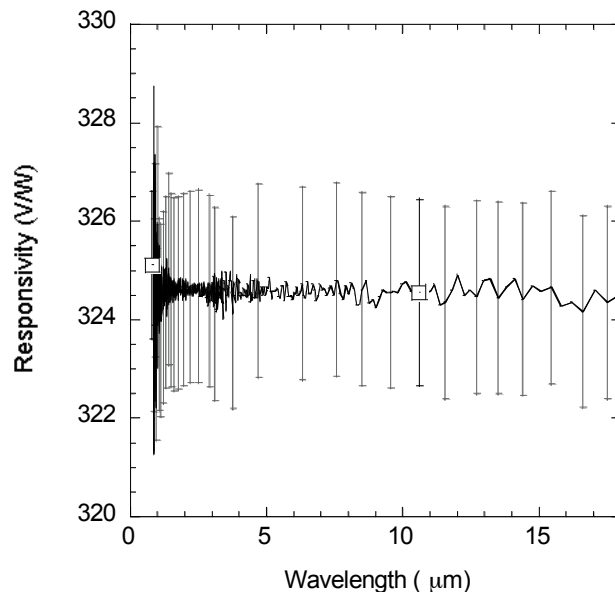


Fig. 10. Spectral power responsivity of the pyroelectric transfer standard Radiometer #2 at 10^9 V/A.

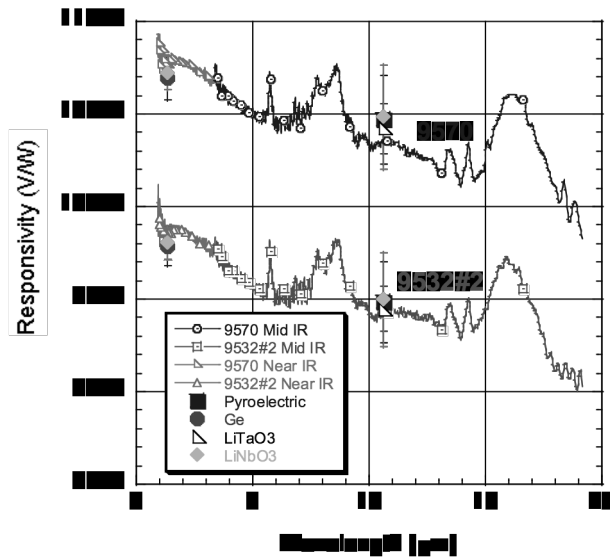


Fig. 11. Spectral power responsivities of the previously calibrated working standard Radiometers 9570 and 9532#2 at 10^{10} V/A signal gains.

responsivity (tie) points with error bars (corresponding to the expanded uncertainties) obtained from laser measurements at $1.32 \mu\text{m}$ and $10.6 \mu\text{m}$. At $1.32 \mu\text{m}$ the working standard pyroelectric radiometers were compared to both Ge and pyroelectric (LiNbO_3) transfer standard radiometers. At $10.6 \mu\text{m}$ the same working standard radiometers were compared to three transfer standard radiometers (pyroelectric LiTaO_3 , LiNbO_3 , and another LiTaO_3). The spectral curves are “tied” to the $1.32 \mu\text{m}$ and $10.6 \mu\text{m}$ responsivity points: i.e. they fall within the error bars at the overlap. The error bars represent the expanded uncertainties. For the $1 \mu\text{m}$ to $19 \mu\text{m}$ spectral range, this was 2.7% ($k = 2$).

The other two working standard pyroelectric radiometers have been calibrated recently. These radiometers have tie points against a Si-trap detector (at 785 nm) and the transfer standard Radiometers #1 and #2 at $10.6 \mu\text{m}$. The spectral power responsivity of the pyroelectric working standard Radiometer P8 is shown as an example in Fig. 12. Its $10.6 \mu\text{m}$ tie point was derived from the transfer standard Radiometer #2 using the detector substitution method. The responsivity is given in V/W at a signal-gain of 10^{10} V/A, where the voltage was derived from the DC (un-chopped) responsivity of the Si-trap detector. The combined relative expanded uncertainties, that include the relative uncertainty of the spectral reflectance measurements of about 0.3% ($k=2$), are also shown with error bars in Fig. 12.

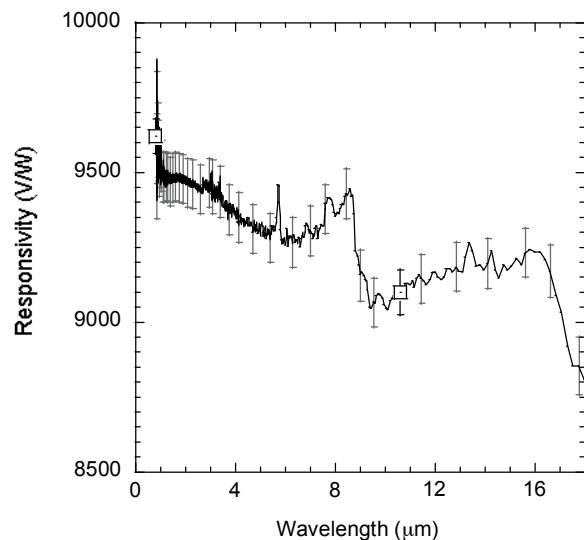


Fig. 12. Spectral power responsivity of the pyroelectric working standard Radiometer P8 at a signal-gain of 10^{10} V/A.

In applications, where these pyroelectric radiometers are used as working standards, the incident beam power at a given wavelength can be calculated from the reading of the lock-in amplifier (attached to the output of the working standard radiometer) divided by the responsivity at the given wavelength. This beam power will be measured by the test devices in a given application.

The uncertainty budget of the spectral power responsivity determination (as an example) for the working standard Radiometer P8 is included in Table 2 at both 785 nm and 10.6 μm . The relative expanded uncertainty of the working standard Radiometer P8 is 0.6 % ($k=2$) at the 785 nm and 0.8 % ($k=2$) at the 10.6 μm tie points. As the uncertainties of the new responsivity tie points were improved, the combined uncertainties of the two newer working standards are about three times lower than the uncertainties of the first two working standards discussed above.

Table 2. Uncertainty budget as an example for the transfer standard pyroelectric Radiometer #2 and the working standard pyroelectric Radiometer P8 at 785 nm and 10.6 μm .

Uncertainty component, Type	Transfer Standard Radiometer #2		Working Std. Radiometer P8	
	785 nm	10.6 μm	785 nm	10.6 μm
Si-trap detector, B	0.20%	0.23%	0.20%	0.30%
Signal variations, A	0.09%	0.05%	0.04%	0.10%
Spatial non-uniformity, B	0.06%	0.09%	0.20%	0.20%
Angular (0-8°) resp. change, B	0.10%	0.10%	0.10%	0.10%
Temperature changes, B	0.02%	0.02%	0.02%	0.02%
Lock-in measurements, B	0.10%	0.10%	0.10%	0.10%
TIS and ray-trace, B		0.08%		
Relative combined std. uncertainty	0.23%	0.29%	0.3%	0.4%
Relative expanded uncertainty ($k=2$)	0.46%	0.58%	0.6%	0.8%

5. CONCLUSIONS

Two transfer standard pyroelectric radiometers have been developed at NIST. As a result of the enhanced absorption from the addition of a reflecting dome above the detector, the Radiometers #1 and #2 have approximately constant radiant power responsivities with less than a variation of 0.4 % and 0.2 %, respectively, between 1 μm and 11 μm , and estimated to be approximately 0.5% for Radiometer #2 out to 18 μm . Additional radiometers with the same design, given knowledge of the bare detector reflectance at longer wavelengths, will not require spectral calibration. One responsivity tie point with low uncertainty is enough to perform the radiometer calibration for the above wavelength range. Four commercial pyroelectric detectors were also calibrated for spectral power responsivity. These radiometers are used as working standards in field applications. They have structured spectral responsivities due to the paint coating. Therefore, spectral reflectance measurements are needed to determine their relative spectral responsivities. A Si tunnel trap detector with a 0.2 % relative expanded uncertainty ($k=2$) was the reference radiometer for both the transfer and the working standard pyroelectric radiometer calibrations.

The domed transfer standard pyroelectric radiometers were used to give the 10.6 μm responsivity tie point for the second set of working standard pyroelectric radiometers with a relative expanded uncertainty of about 0.6 % ($k=2$). The combined relative expanded uncertainties of the recently calibrated working standard pyroelectric radiometers were about 1 % ($k=2$) between 1 μm and 18 μm .

6. ACKNOWLEDGEMENT

The authors thank John Lehman for developing the high performance pyroelectric detectors used in the transfer standard radiometers described in this paper.

REFERENCES

1. Eppeldauer, G.P., Racz, M., and Hanssen, L.M., *Spectral responsivity determination of a transfer-standard pyroelectric radiometer*. SPIE Proceedings, 2002. **4818**: p. 118-126.
2. Eppeldauer, G.P., et al., *Spectral irradiance responsivity measurements between 1 μm and 5 μm* . SPIE proceedings, 2004. **5543**(Society of Photo-Optical Instrumentation Engineers): p. 248-257.
3. Eppeldauer, G.P. and Racz, M., *Spectral Power and irradiance responsivity calibration of InSb working standard radiometers*. Appl. Opt., 2000. **39**(31): p. 5739-5744.
4. Gong, H., Hanssen, L.M., and Eppeldauer, G.P., *Spatial and angular responsivity measurements of photoconductive HgCdTe LWIR radiometers*. Metrologia, 2004. **41**: p. 161-166.
5. Lehman, J., et al., *Domain-engineered pyroelectric radiometer*. Appl. Opt., 1999. **38**(34): p. 7047-7055.
6. Day, G.W., Hamilton, A., and Pyatt, K.W., *Spectral reference detector for the visible to 12- micrometer region; convenient, spectrally flat*. Appl. Opt., 1976. **15**(7): p. 1865-1868.
7. Fox, N.P., Prior, T.R., and Theocharous, E., *Radiometric calibration of infrared detectors and thermal imaging systems*. SPIE Proceedings, 1995. **2474**: p. 229-237.
8. Eppeldauer, G.P., et al., *Realization of a spectral radiance responsivity scale with a laser-based source and Si radiance meters*. Metrologia, 2000. **37**: p. 531-534.
9. Larason, T.C., Bruce, S.S., and Parr, A.C. *Spectroradiometric detector measurements*. NIST Special Publication, 1998. **250-41**.
10. Gentile, T.R., et al., *Calibration of a pyroelectric detector at 10.6 μm with the NIST High-Accuracy Cryogenic Radiometer*. Appl. Opt., 1997. **36**: p. 3614-3621.